

Ex-framework FeZSM-5 for control of N₂O in tail-gases

Javier Pérez-Ramírez^{a,*}, Freek Kapteijn^b, Guido Mul^b,
Xiaoding Xu^b, Jacob A. Moulijn^b

^a Norsk Hydro, Research Centre, Hydrocarbon Processes and Catalysis, P.O. Box 2560, N-3907 Porsgrunn, Norway

^b Reactor & Catalysis Engineering, DelftChemTech, Delft University of Technology, Julianalaan 136, 2628 BL Delft, The Netherlands

Abstract

In this paper, the performance of a novel ex-framework FeZSM-5 catalyst for direct N₂O decomposition in simulated tail-gas from nitric acid plants (containing O₂, NO_x, and H₂O) and combustion processes (containing O₂, CO₂, H₂O, and SO₂) is presented. This catalyst was prepared by isomorphous substitution of Fe in the MFI framework followed by calcination and steam activation. The specific activity per mole of Fe of the ex-framework catalyst in N₂O/He was 4–10 times higher than observed for FeZSM-5 catalysts prepared by conventional solid and liquid-ion exchange and sublimation methods. The presence of NO_x and SO₂ has a positive effect on the N₂O conversion over ex-FeZSM-5, decreasing the inhibition effect of H₂O, while O₂ and CO₂ do not influence catalytic performance. The operation temperature is decreased ~100 K by addition of propene to the feed mixture. The stability of ex-framework FeZSM-5 for direct N₂O decomposition, in the absence of any reductant, was remarkable, showing no significant deactivation (at N₂O conversion levels ranging from 20 to 65%) after 600 h time-on-stream. Sublimed and especially ion-exchanged FeZSM-5 catalysts showed a strong irreversible deactivation in feed mixtures containing H₂O and SO₂. The performance of the ex-framework catalyst has also been compared with that of different Rh-based catalysts. Co–Rh, Al mixed oxide, derived from a hydrotalcite precursor containing these metals, shows a remarkably high N₂O decomposition activity in N₂O/He. The initial activity of this catalyst in a simulated tail-gas mixture is higher compared to ex-FeZSM-5, but is severely inhibited by NO and deactivated in the presence of H₂O and SO₂. This also applies to other Rh-based catalysts. Application of ex-framework FeZSM-5 appears to allow a flexible and cost-effective *end-of-pipe* catalytic technology in chemical production plants and combustion processes. Different abatement options have been considered, depending on the source and the operating conditions of the process. Aspects of (monolithic) reactor design for an optimal catalyst implementation are also discussed.

© 2002 Elsevier Science B.V. All rights reserved.

Keywords: N₂O; Decomposition; Reduction; Greenhouse effect; FeZSM-5; Ex-framework; Tail-gas; Nitric acid; Combustion; Reactor; Fixed bed; Monolith

1. Introduction

Nitrous oxide (N₂O) has been identified as a greenhouse gas and a significant contributor to the

destruction of ozone in the stratosphere [1–4]. N₂O is produced by both natural and anthropogenic sources. Agriculture is a major anthropogenic source, but control of these emissions is difficult due to the very diffuse nature of N₂O emissions. The major industrial source of N₂O is the production of nitric acid (400 kt N₂O per year), which is a key bulk chemical in the fertilizer industry [5]. N₂O is also produced during the manufacture of adipic acid,

* Corresponding author. Tel.: +47-35-92-76-73;
fax: +47-35-92-47-38.
E-mail address: javier.perez.ramirez@hydro.com
(J. Pérez-Ramírez).

caprolactam, acrylonitrile, glyoxal, and in general organic syntheses using HNO_3 as the oxidant or reactions involving ammonia oxidation. Nitric acid production facilities, e.g. in the Netherlands contribute to 25 kt N_2O per year [6], i.e. $\sim 6\%$ of the global N_2O emission related to nitric acid plants. Reduction of these emissions will lead to 35% reduction of the 6% committed in Kyoto in December, 1997. The emission of the chemical process industry is concentrated in a limited number of large nitrous oxide sources, which holds the promise for an economic and efficient reduction strategy. Combustion processes of fossil fuels, biomass, and waste in fluidized-bed combustors also contribute significantly to N_2O emissions [5–7], although quantification is less accurate.

Emissions associated with nitric acid plants and stationary combustion processes are characterized by concentrations of N_2O in the tail-gas below 1 vol.% and typically in the 0.05–0.2 vol.% range [7,8]. Different (thermal and catalytic) abatement technologies have been successfully developed for the other major industrial source, i.e. adipic acid plants [9,10], but these are not applicable to nitric acid plants or combustion processes [7,8,11]. In adipic acid plants, due to the high N_2O concentration in the tail-gas (25–40 vol.%) and the exothermicity of the N_2O decomposition reaction, a large increase in the temperature occurs within the catalyst bed. For instance, the decomposition of N_2O contained in a gas at 35 vol.% of N_2O in He leads to an adiabatic temperature rise of the gas of 938 K. In this temperature window, a large number of catalysts exhibit considerable activity. So, in this case, the activity of the catalyst is not a critical factor for the effectiveness of the technology.

In general, direct catalytic decomposition of N_2O into N_2 and O_2 is an attractive option to reduce N_2O emissions, but none of the catalysts proposed in the literature show a good activity and stability in N_2O conversion under realistic conditions of feed composition and space velocities [8,11]. Transition (Cu, Co, Ni) and noble-metal based catalysts (Rh, Ru, Pd) on different supports (ZnO, CeO_2 , Al_2O_3 , TiO_2 , ZrO_2 , or calcined hydrotalcites) are very active for N_2O decomposition in $\text{N}_2\text{O}/\text{He}$ feeds, but the presence of other gases in the feed (NO_x , H_2O , SO_2) leads to strong inhibition and/or deactivation [12–21].

FeMFI is an interesting catalytic system because N_2O conversion shows anomalous behavior in the presence of tail-gas components compared to other catalytic systems [12,22–24]. Different preparation methods have been reported to optimize the catalytic performance of FeZSM-5, not only in N_2O decomposition [25–27], but also in de- NO_x HC-SCR and selective oxidations [28–32]. The methods normally applied include solid- and liquid-ion exchange, or sublimation. From the different results in the literature, it is concluded that the development and optimization of preparation routes to prepare FeZSM-5 may lead to improved catalyst performance in the different processes catalyzed by this material [23,25,27,30]. Several authors have claimed a good stability of FeMFI catalysts prepared by sublimation and (aqueous) ion-exchanged for N_2O reduction in the presence of H_2O and/or SO_2 [8,26,27,33,34]. This behavior is induced by the co-addition of light hydrocarbons (methane, propane, propene, or LPG) as a reductant in the feed mixture, which also lowers the light-off temperature for N_2O decomposition. Other authors also claimed that the use of reductant (hydrocarbon or ammonia) over Fe-zeolites reduces N_2O and NO emissions simultaneously [28,35], but the catalysts do not exhibit sufficient activity due to different operation temperatures of both processes. The addition of reductant is not attractive in tail-gas abatement units due to the high operation cost associated. Data on stability of FeZSM-5 catalysts for direct N_2O decomposition (without addition of reductant) in simulated tail-gases is hardly available [23,24].

In this paper we present a high activity and stability of a FeZSM-5 catalyst prepared via an ex-framework route in direct N_2O decomposition in simulated tail-gases (containing O_2 , CO_2 , NO_x , SO_2 , and H_2O) at high space velocities ($36\,000\text{--}120\,000\text{ h}^{-1}$). The catalytic behavior of ex-framework FeZSM-5 is compared with FeZSM-5 catalysts prepared by (solid and liquid) ion-exchange and sublimation methods and with Rh-based catalysts on different supports, including Al_2O_3 , ZSM-5, USY, and calcined hydrotalcites. The implementation of this catalytic technology for N_2O abatement in different sources is presented, including the analysis of various process options and aspects of reactor design.

2. Experimental

2.1. Catalyst preparation

2.1.1. FeZSM-5 catalysts

Isomorphously substituted FeZSM-5 was synthesized hydrothermally using TPAOH as the template [32]. The as-synthesized samples were calcined in air atmosphere at 825 K for 10 h and converted into the H-form by three consecutive exchanges with a NH_4NO_3 solution (0.1 M) (denoted as FeZSM-5c). Finally, the catalysts were activated in flowing steam at ambient pressure (water partial pressure of 300 mbar and $30 \text{ ml (STP) min}^{-1}$ of N_2 flow) at 875 K during 5 h (denoted as ex-FeZSM-5). Other FeZSM-5 catalysts were prepared by solid-ion exchange with $\text{FeCl}_2 \cdot 4\text{H}_2\text{O}$ (sie-FeZSM-5) and liquid (aqueous) ion-exchange with $\text{Fe}(\text{NO}_3)_3 \cdot 9\text{H}_2\text{O}$ (lie-FeZSM-5), following conventional procedures described in the literature [28,29]. $\text{NH}_4\text{-ZSM-5}$ (CBV 8020; Zeolyst) was used as the parent zeolite. Sub-FeZSM-5 was prepared by sublimation of FeCl_3 on H-ZSM-5 (Degussa), according to the method described elsewhere [30].

2.1.2. Rh-based catalysts

Rh/ Al_2O_3 , Ru/ZSM-5, and Rh/USY were prepared by incipient wetness method, using appropriate solutions of $\text{Rh}(\text{NO}_3)_3$. Al_2O_3 (CK 300, Ketjen), $\text{NH}_4\text{-ZSM-5}$ (CBV 8020; Zeolyst), H-USY (CBV 720; Zeolyst) were used as supports. After the impregnation procedure, the samples were dried at 375 K for 5 h and calcined in static air at 825 K. Ex-Co-Rh,Al-HTlc was prepared by coprecipitation at constant pH and temperature at low saturation conditions and thermal decomposition in static air at 725 K for 18 h [19,20].

2.2. Catalyst characterization

The chemical composition of the samples was determined by ICP-OES in a Perkin-Elmer Plasma 40 (Si) and Optima 3000DV (axial). The total pore volume of the samples was determined by N_2 adsorption at 77 K (Autosorb 6B). Prior to the measurements the samples were evacuated at 625 K for 16 h. The surface area was determined using the BET method. TEM analysis was carried out on a Philips CM 30

T electron microscope. Rh dispersion in the catalysts (D_{Rh}) was determined by CO-chemisorption using a volumetric apparatus (QuantaChrome Autosorb 1-C), assuming an adsorption stoichiometry $\text{Rh}:\text{CO} = 1:1$. Prior to chemisorption, the sample was reduced in H_2 (775 K, 1 h), followed by evacuation (775 K, 2 h) and cooling to room temperature in vacuum.

2.3. Activity test

Activity and stability tests were carried out in a six-flow reactor system [36]. Tests were made using 50 mg of catalyst shaped in particles with diameters of 125–250 μm and space velocities ranging from 36 000 to 120 000 h^{-1} . Total pressure P was 3 bar. The partial feed pressure of the different gases depends on the tail-gas simulated:

- *Nitric acid plants.* 4.5 mbar N_2O , 20 mbar O_2 , 1 mbar NO, 15 mbar H_2O , balance He. C_3H_6 (4.5 mbar) was eventually added to the complete feed mixture. Experiments varying the partial feed pressure of NO (0–4.5 mbar) were also carried out.
- *Combustion processes.* 1.5 mbar N_2O , 120 mbar O_2 , 150 mbar CO_2 , 90 mbar H_2O , 0.75 mbar SO_2 , balance He.

Individual and combined effects of these gas mixtures on the catalytic activity were investigated. For the assessment of the effect of individual gases on the N_2O conversion, fresh catalysts were used in every test. Before reaction, the catalysts were pretreated in 4.5 mbar N_2O (tail-gas from nitric acid production) or 1.5 mbar N_2O (tail-gas from combustion processes) in He at 725 K for 1 h and cooled down in the same gas to the starting reaction temperature. Generally, 1 h after a change of conditions the conversion levels for the different gases were constant and considered in steady state. Preliminary checks were made to ensure the absence of diffusion limitations on the reaction rate [36]. At least two analyses were averaged for a data point. The product gases were continuously analyzed with a chemiluminescence NO– NO_2 analyzer (Ecophysics CLD 700 EL), and discontinuously analyzed for the other gases by GC (Chrompack CP 9001). The chromatograph was equipped with a thermal conductivity detector and a flame ionization detector, using a Poraplot Q column (for N_2O , C_3H_6 , and CO_2 separation) and a Molsieve 5A column (for N_2 , O_2 , and CO

separation). The mass balance for N, O, and C in these experiments closed within less than 1, 2, and 5%, respectively.

3. Results and discussion

3.1. Activity in N_2O/He

Table 1 shows the characterization results of the FeZSM-5 catalysts used in this study. The Fe content in ex-FeZSM-5 is about three and eight times higher in the ion-exchanged catalysts (~ 1.5 wt.%) and sublimed catalyst (5 wt.%), respectively. Fig. 1 shows that sub-FeZSM-5 and ex-FeZSM-5 induce similar absolute N_2O conversion levels in a N_2O/He feed and significantly higher conversion levels than the ion-exchanged catalysts. The sie-FeZSM-5 is more active than lie-FeZSM-5. Calculation of the turnover frequency (TOF), i.e. the specific activity for N_2O decomposition per mole of (total) iron at different reaction temperatures gives a clear indication of the iron utilization in the catalysts (Fig. 2). At, e.g. 700 K, this value is more than four, seven, and 10 times higher for ex-FeMFI than for sie-FeZSM-5, sub-FeZSM-5, and lie-FeZSM-5, respectively. Activation of the calcined FeZSM-5c sample with steam at 875 K is crucial to

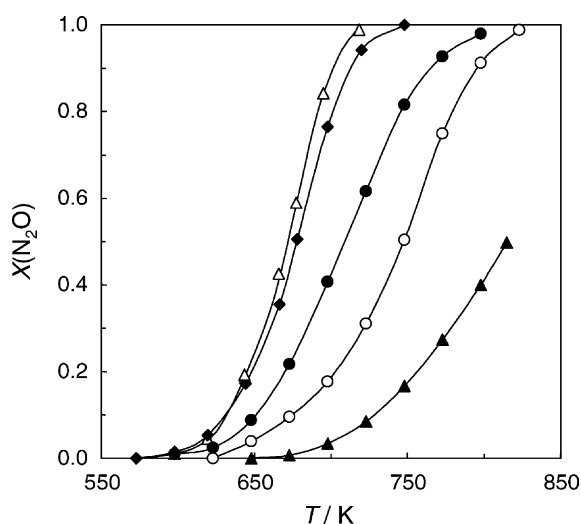


Fig. 1. N_2O conversion vs. T over (◆) ex-FeZSM-5, (▲) FeZSM-5c (before steaming), (●) sie-FeZSM-5, (○) lie-FeZSM-5, and (△) sub-FeZSM-5. Conditions: 4.5 mbar N_2O in He; $P = 3$ bar; GHSV = 36 000 h^{-1} .

create active species in the ex-framework catalyst, as can be concluded by comparison of the activity curves of both calcined and steamed samples in Fig. 1.

Fig. 3 shows the N_2O conversion vs. temperature curve of different Rh-catalysts in a N_2O/He feed at

Table 1
Data of the catalysts used in this study

Catalyst	FeZSM-5 catalysts				
	Si/Al ^a	Fe ^a (wt.%)	V_{pore}^b ($\text{cm}^3 \text{g}^{-1}$)	S_{BET}^b ($\text{m}^2 \text{g}^{-1}$)	Δd^c (nm)
Ex-FeZSM-5	31.5	0.58	0.22	395	1–2
Sie-FeZSM-5	37.5	1.46	0.27	370	5–15
Lie-FeZSM-5	37.5	1.50	0.28	375	7–25
Sub-FeZSM-5	14.0	5.0	0.30	–	3–12
Rh-based catalysts					
	M/Al ^d	Rh ^a (wt.%)	V_{pore}^b ($\text{cm}^3 \text{g}^{-1}$)	S_{BET}^b ($\text{m}^2 \text{g}^{-1}$)	D_{Rh}^e (%)
Rh/Al ₂ O ₃	–	1.05	0.63	280	60
Rh/ZSM-5	37.5	0.99	0.26	372	25
Rh/USY	16.0	1.10	0.45	690	33
Ex-Co–Rh,Al-HTlc	2.9	0.73	0.80	150	>80

^a ICP-OES.

^b N_2 adsorption at 77 K.

^c Size distribution of iron oxide particles, as determined from TEM.

^d Metal molar ratio: Si/Al in zeolites, and Co/Al in the mixed oxide.

^e Dispersion, from CO-chemisorption.

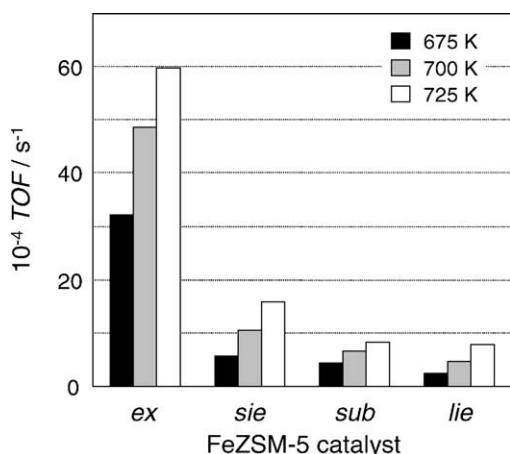


Fig. 2. TOF values (moles of N_2O converted per mole of Fe s^{-1}) for the different FeZSM-5 catalysts, determined after 1 h time-on-stream. Conditions: 4.5 mbar N_2O in He; $P = 3$ bar; GHSV = $60\,000\text{ h}^{-1}$.

$60\,000\text{ h}^{-1}$. The activity curve of ex-FeZSM-5 at the same experimental conditions is also displayed for comparative purposes. The temperature for a certain N_2O conversion differs $\sim 300\text{ K}$ between ex-Co-Rh,Al-HTlc (the most active catalyst in our experiments) and ex-FeZSM-5. The activity of the Rh-catalysts is influenced by the support, following

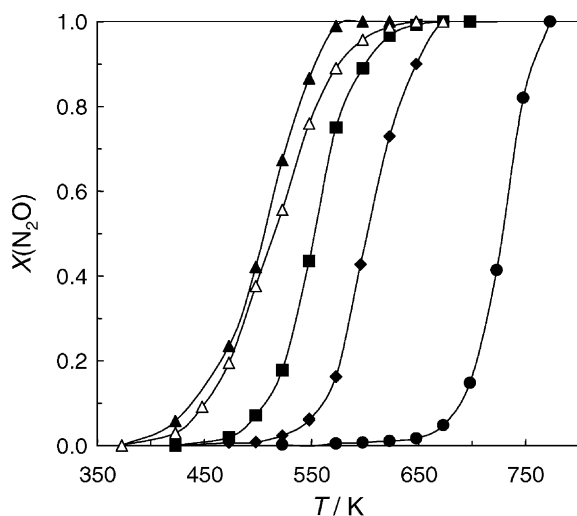


Fig. 3. N_2O conversion vs. T over (●) ex-FeZSM-5, (◆) Rh/ZSM-5, (■) Rh/USY, (△) Rh/Al₂O₃, and (▲) ex-Co-Rh,Al-HTlc. Conditions: 4.5 mbar N_2O in He; $P = 3$ bar; GHSV = $60\,000\text{ h}^{-1}$.

the sequence: ex-Co-Rh, Al-HTlc \geq Rh/Al₂O₃ > Rh/USY > Rh/ZSM-5. The activity data suggest a correlation between the Rh dispersion in the catalyst and the N_2O conversion: the higher the Rh dispersion (see Table 1), the higher the N_2O decomposition activity. These results are in agreement with previous studies over Rh-catalysts [37], where the influence of both support and Rh precursor in the N_2O decomposition activity was investigated. The metal dispersion of ex-Co-Rh,Al-HTlc was not determined by CO-chemisorption, because during the pretreatment in H_2 a significant fraction of Co is reduced, leading to overestimation of the amount of Co adsorbed (apparent dispersion > 100%). No Rh-related particles were observed in the TEM analysis of the sample, which suggests a particle size of <1 nm, leading to dispersions of >80%, as expressed in Table 1. The high dispersion of Rh in the mixed oxide is a consequence of the preparation method via a hydrotalcite precursor and an optimized decomposition temperature, based on previous investigations with in situ infrared and Raman spectroscopies [38–40].

3.2. Performance in simulated tail-gases

3.2.1. Nitric acid plants

The performance of ex-FeZSM-5 in simulated tail-gas from nitric acid plants (containing N_2O and O_2 , NO, and H_2O) is shown in Fig. 4. N_2O conversion was measured after 1 h time-on-stream in a specific feed composition. Ex-FeZSM-5 shows a substantial N_2O conversion above 700 K in a $\text{N}_2\text{O}/\text{He}$ feed. Addition of O_2 to the feed hardly affects the activity, while NO enhances the reaction rate considerably. Apparently, molecular oxygen does not dissociate over FeZSM-5 and does not compete with N_2O for active sites. NO promotes N_2O conversion by accelerating the desorption rate of adsorbed O^* species (deposited by N_2O decomposition). The mechanism of this catalytic reaction has been described in detailed elsewhere [41]. Water severely inhibits the reaction, probably by hydroxylation of the active sites and adsorption in the zeolite channels. Nevertheless, in the complete gas mixture ($\text{N}_2\text{O} + \text{O}_2 + \text{NO} + \text{H}_2\text{O}$), ex-FeZSM-5 still shows a significantly higher activity than in N_2O alone (100% conversion at 750 K). The promoting effect of NO is thus stronger than the inhibition by H_2O .

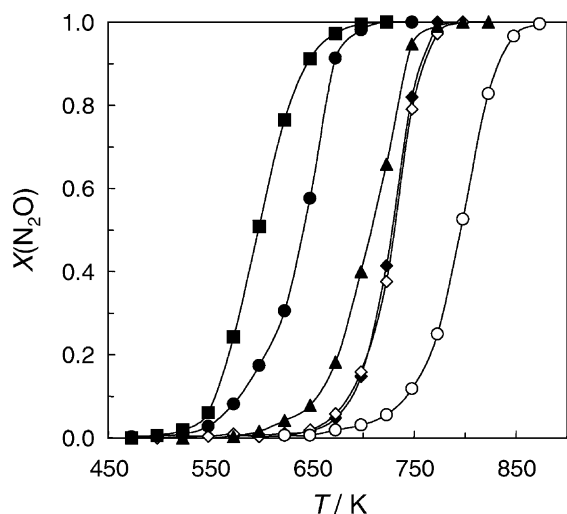


Fig. 4. N_2O conversion vs. T over ex-FeZSM-5 in simulated tail-gases from nitric acid plants. Conditions: (\blacklozenge) 4.5 mbar N_2O , (\diamond) 4.5 mbar N_2O + 70 mbar O_2 , (\bullet) 4.5 mbar N_2O + 1 mbar NO , (\circ) 4.5 mbar N_2O + 15 mbar H_2O , (\blacktriangle) 4.5 mbar N_2O + 70 mbar O_2 + 1 mbar NO + 15 mbar H_2O , (\blacksquare) 4.5 mbar N_2O + 70 mbar O_2 + 1 mbar NO + 15 mbar H_2O + 4.5 mbar C_3H_6 , balance He; $P = 3$ bar; $\text{GHSV} = 60\,000\text{ h}^{-1}$.

This extraordinary behavior distinguishes ex-framework FeZSM-5 from other N_2O decomposition catalysts. Fig. 5 shows the individual and combined effect of the different gases on the N_2O conversion over ex-Co-Rh,Al-HTlc. In this case, the N_2O conversion was not affected by oxygen, but the presence of NO severely inhibits the reaction, probably via surface nitrite/nitrate formation, shifting the reaction to 200 K higher temperatures. The inhibition effect of water is even more severe than that of NO. A similar trend was observed for the other Rh-catalysts. As a result of these inhibition effects, the operation temperature of the Rh-based catalysts is similar to that of ex-framework FeZSM-5 (Fig. 6) in simulated tail-gas conditions. It should be mentioned that the activity of ex-Co-Rh,Al-HTlc in terms of absolute conversion at a certain temperature is significantly higher than observed for the other catalysts, e.g. N_2O conversion in the complete feed mixture over ex-Co-Rh,Al-HTlc and ex-FeZSM-5 at 700 K is 70 and 40%, respectively.

The temperature of N_2O decomposition over ex-FeZSM-5 can be further decreased by the addition of hydrocarbons to the feed (selective catalytic

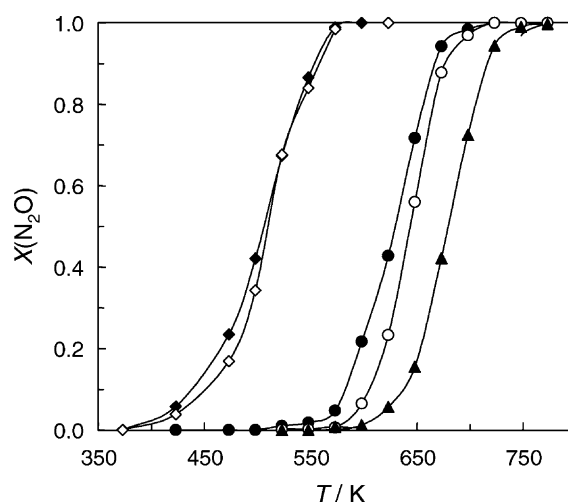


Fig. 5. N_2O conversion vs. T over ex-Co-Rh,Al-HTlc in simulated tail-gases from nitric acid plants. Conditions: (\blacklozenge) 4.5 mbar N_2O , (\diamond) 4.5 mbar N_2O + 70 mbar O_2 , (\bullet) 4.5 mbar N_2O + 1 mbar NO , (\circ) 4.5 mbar N_2O + 15 mbar H_2O , ($\%$) 4.5 mbar N_2O + 70 mbar O_2 + 1 mbar NO + 15 mbar H_2O , balance He; $P = 3$ bar; $\text{GHSV} = 60\,000\text{ h}^{-1}$.

reduction). Addition of 4.5 mbar of propene (molar $\text{N}_2\text{O}/\text{C}_3\text{H}_6$ feed ratio of 1) leads to a reduction in temperature of 100 K in the simulated tail-gas, achieving 100% N_2O conversion at 675 K (Fig. 4). Addition of

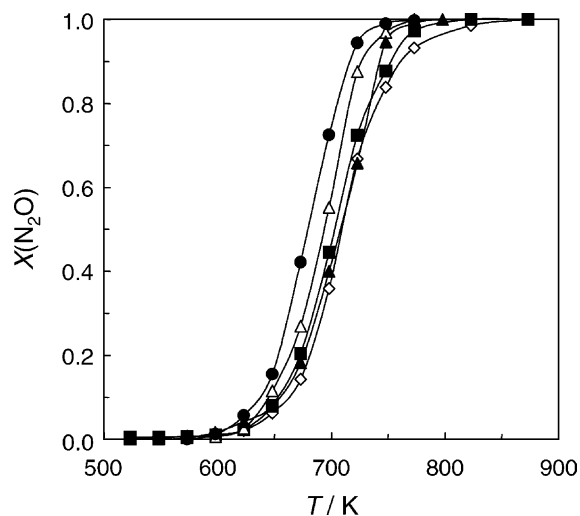


Fig. 6. N_2O conversion vs. T over (\blacktriangle) ex-FeZSM-5, (\bullet) ex-Co-Rh,Al-HTlc, (\triangle) Rh/ Al_2O_3 , (\blacksquare) Rh/USY, and (\diamond) Rh/ZSM-5. Conditions: 4.5 mbar N_2O + 70 mbar O_2 + 1 mbar NO + 15 mbar H_2O , balance He; $P = 3$ bar, $\text{GHSV} = 60\,000\text{ h}^{-1}$.

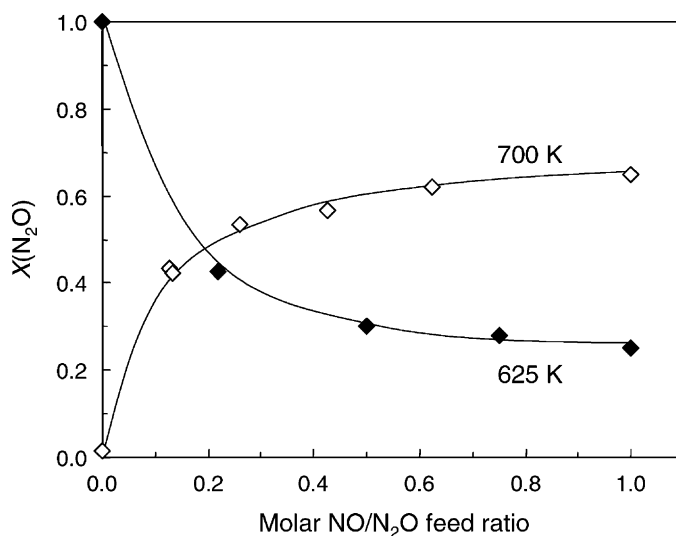


Fig. 7. N₂O conversion vs. molar NO/N₂O feed ratio over (◇) ex-FeZSM-5 and (◆) ex-Co-Rh,Al-HTlc at the temperatures indicated in the figure. Conditions: 4.5 mbar N₂O and 0–4.5 mbar NO, balance He; $P = 3$ bar; GHSV = 60 000 h⁻¹.

propene does not influence the N₂O conversion over Rh-catalysts, since Rh shows a high activity for oxygen activation [42]. This facilitates the combustion of propene at lower temperatures than those needed for activation of N₂O.

The activity measurements shown in Figs. 4 and 5 indicate a remarkable opposite effect of NO in ex-FeZSM-5 (promoting) and ex-Co-Rh,Al-HTlc (and in general other Rh-based catalysts, inhibiting). Fig. 7 shows the N₂O conversion at different molar NO/N₂O feed ratios in both catalytic systems. Ex-FeZSM-5 shows a dramatic improvement in N₂O conversion upon addition of NO, while the conversion over ex-Co-Rh,Al-HTlc is strongly inhibited. Both promotion and inhibition effects are especially significant after addition of small amounts of NO to the feed, i.e. at molar NO/N₂O feed ratios <0.2. NO inhibition over ex-Co-Rh,Al-HTlc was completely reversible, since the original conversion was obtained in less than 1 h after removing NO from the feed mixture.

The remarkable behavior of ex-FeZSM-5 in simulated tail-gas mixtures is not limited to its activity, but also includes stability. N₂O conversion over ex-FeZSM-5 exhibits a remarkable stability during 50 h in the complete feed mixture (excluding the hydrocarbon) at different space velocities, ranging

from 36 000 to 120 000 h⁻¹ (Fig. 8). Sub-FeZSM-5 shows slight deactivation at 36 000 h⁻¹. Significant deactivation was observed for the sie-FeZSM-5 and lie-FeZSM-5 catalysts.

In a more severe stability test during 600 h, the stability of ex-FeZSM-5 and ex-Co-Rh,Al-HTlc have been compared (Fig. 9). The ex-framework catalyst shows a remarkable stability along the experiment at 675 and 725 K. As it was already shown in Fig. 4, the N₂O conversion in the tail-gas mixture (excluding the hydrocarbon) is higher than in a N₂O/He feed over this catalyst. N₂O conversion over ex-Co-Rh,Al-HTlc at 675 K is stable during the first 25 h, but afterwards the activity decreases significantly. After 300 h, the catalyst has lost ~60% of the original activity. After switching the tail-gas mixture to a mixture of N₂O in He, the conversion measured was 80%, which indicates certain deactivation, since in the activity test shown in Fig. 5 the N₂O conversion was 100% under these experimental conditions. Since NO inhibition over the Rh-catalysts is reversible, it can be suggested that water is responsible for deactivation of these formulations. After exposing the catalyst to the complete tail-gas mixture (>400 h) the conversion rapidly decreases up to the level at 300 h and slowly decreases with time. This deactivation behavior, being typical in the different Rh-catalysts tested in this study, limits

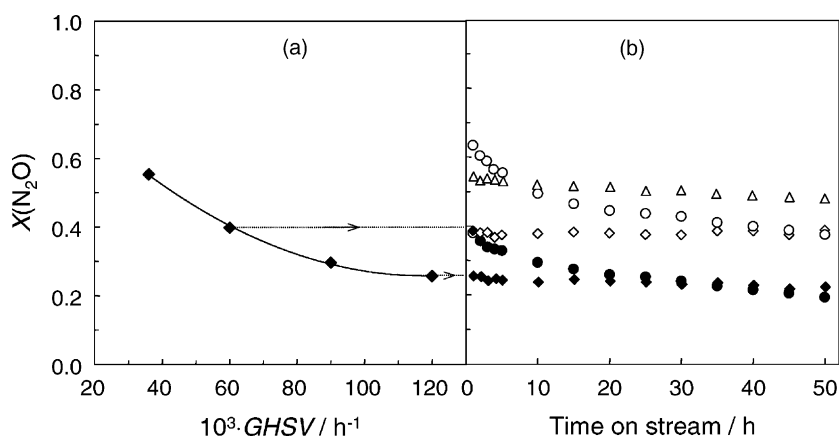


Fig. 8. N_2O conversion as a function of (a) the space velocity (GHSV) over ex-FeZSM-5 and (b) time-on-stream over (\diamond) ex-FeZSM-5 (60 000 h^{-1} , 700 K), (\blacklozenge) ex-FeZSM-5 (120 000 h^{-1} , 700 K), (\bullet) sie-FeZSM-5 (36 000 h^{-1} , 725 K), (\circ) lie-FeZSM-5 (36 000 h^{-1} , 775 K), and (\triangle) sub-FeZSM-5 (36 000 h^{-1} , 700 K). Conditions: 4.5 mbar N_2O + 70 mbar O_2 + 1 mbar NO + 15 mbar H_2O , balance He.

their practical application in catalytic N_2O abatement in tail-gases from nitric acid plants.

The catalysts presented in this paper were the most promising over an extensive screening program (not shown here). Catalysts based on other metals like Ru, Pd, Co, and Ni on different supports also exhibit high activities in $\text{N}_2\text{O}/\text{He}$ feeds, but all of them present a poor performance in simulated tail-gas conditions. In all these cases, even the presence of oxygen inhibits the reaction significantly.

3.2.2. Combustion processes

The performance of ex-FeZSM-5 in simulated tail-gases from combustion processes (containing N_2O and O_2 , CO_2 , H_2O , and SO_2) at 75 000 h^{-1} is shown in Fig. 10. A substantial conversion above 700 K in a $\text{N}_2\text{O}/\text{He}$ feed is obtained. Analogously to the former activity tests, addition of O_2 does not affect the activity, while water causes severe inhibition. CO_2 , a common constituent of tail-gas in combustion processes, did not influence the performance of the catalyst. The catalytic activity is enhanced considerably by the presence of SO_2 in the feed. In the complete gas mixture ($\text{N}_2\text{O} + \text{O}_2 + \text{CO}_2 + \text{H}_2\text{O} + \text{SO}_2$), ex-FeZSM-5 shows N_2O conversions of 90% at 800 K, which is somewhat lower than in the $\text{N}_2\text{O}/\text{He}$ mixture. In this case, the promoting effect of SO_2 does not compensate the strong inhibition of H_2O . Small amounts of SO_2 in the feed (~ 50 ppm) completely

suppress the activity in N_2O decomposition of Rh-catalysts, and the effect is completely irreversible. The original activity was not recovered even after regeneration of the catalyst in air at 775 K. Again, this makes the application of noble-metal based catalysts from a practical point of view very unattractive.

The resistance of ex-FeZSM-5 to deactivation by SO_2 and H_2O is remarkable. Stability is a crucial requirement for application of catalytic after-treatment in combustion facilities, even when catalysts maintain mild activity. N_2O conversion over ex-FeZSM-5 exhibits a significant stability in the complete feed mixture at 75 000 h^{-1} (Fig. 11). After switching from $\text{N}_2\text{O}/\text{He}$ to the complete tail-gas mixture at 740 K, the N_2O conversion gradually decreases during the first 75 h, obtaining stable behavior afterwards. After ~ 200 h on stream, the feed gas was switched back to $\text{N}_2\text{O}/\text{He}$. N_2O conversion rapidly increases (black diamonds, Fig. 11), and the original N_2O conversion was practically recovered after 5 h. At 760 and 780 K, a very stable behavior is observed in simulated tail-gas for both catalysts, with no sign of deactivation. Additionally, the inhibition by the feed mixture is completely reversible. This result is particularly remarkable if one realizes that the SO_2 pressure used in this study corresponds to 750 ppm SO_2 under atmospheric flue-gas conditions, which typically contains only 10–50 ppm SO_2 . The total amount of SO_2 passed over the catalysts during the 600 h experiments

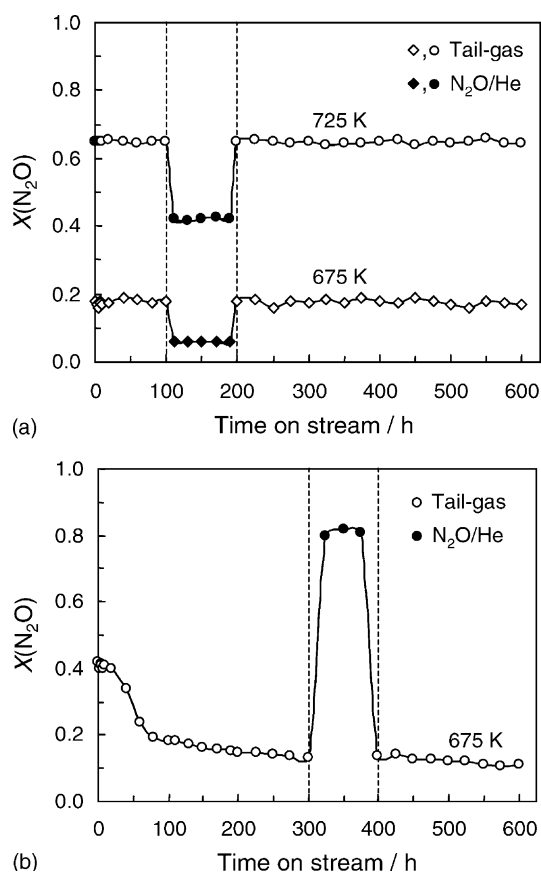


Fig. 9. N_2O conversion vs. time-on-stream over (a) ex-FeZSM-5 and (b) ex-Co-Rh,Al-HTlc in (●, ◆) 4.5 mbar N_2O and (○, ◇) 4.5 mbar N_2O + 70 mbar O_2 + 1 mbar NO + 15 mbar H_2O , balance He; $P = 3$ bar; GHSV = $60\,000\text{ h}^{-1}$. Temperatures are as indicated in the figure.

(Fig. 11) corresponds to an amount of SO_2 emitted by a conventional combustion facility over more than 1 year, at 50 ppm levels.

The catalysts prepared by the ion-exchanged and sublimation methods were further investigated at three different temperatures and exposure times in $\text{N}_2\text{O}/\text{He}$ (bars A and E in Fig. 12) and in the simulated feed mixture (bars B, C, and D in Fig. 12). This figure shows the following: (i) there is a significant reduction of N_2O conversion by changing the gas composition from $\text{N}_2\text{O}/\text{He}$ to the tail-gas mixture (compare bars A and B at different temperatures); (ii) activity progressively decreases with exposure time (1, 5, and 20 h) to the simulated feed mixture (compare bars B, C, and

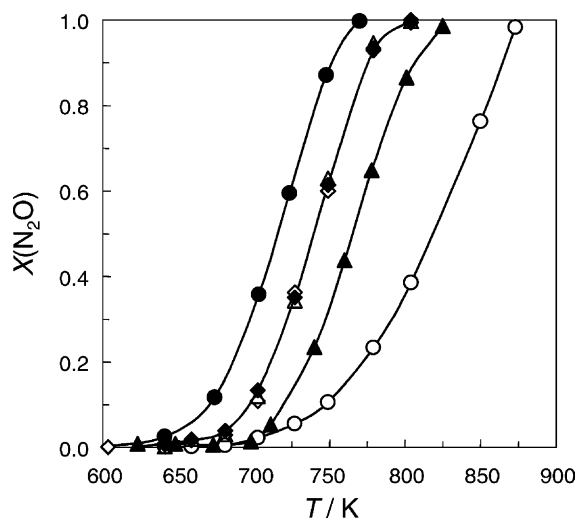


Fig. 10. N_2O conversion vs. T over ex-FeZSM-5 in simulated tail-gases from combustion processes. Conditions: (◆) 1.5 mbar N_2O , (◇) 1.5 mbar N_2O + 120 mbar O_2 , (△) 1.5 mbar N_2O + 150 mbar CO_2 , (○) 1.5 mbar N_2O + 90 mbar H_2O , (●) 1.5 mbar N_2O + 0.75 mbar SO_2 , (▲) 1.5 mbar N_2O + 120 mbar O_2 + 150 mbar CO_2 + 90 mbar H_2O + 0.75 mbar SO_2 , balance He; $P = 3$ bar; GHSV = $75\,000\text{ h}^{-1}$.

D); (iii) sub-FeZSM-5 is much less affected by changing the feed composition than the ion-exchanged catalysts, while lie-FeZSM-5 is the most sensitive formulation to the feed composition; (iv) the catalysts show irreversible deactivation, i.e. N_2O conversion does not reach the original level after removal of the additional gas components in the feed mixture (compare bars A and E at different temperatures). The irreversible deactivation is especially remarkable in lie-FeZSM-5, while sie-FeZSM-5 and especially sub-FeZSM-5 recover a significant fraction of their original activity after removing H_2O and SO_2 from the feed mixture. The poor activity and stability of the ion-exchanged samples is not related only to the formation of stable sulfates in the catalyst surface. Also H_2O was found to depress the activity over these catalytic systems.

When SO_2 is present in the feed, most of the catalysts for N_2O decomposition rapidly deactivate [7,8,11,16,17,19]. It is proposed that the SO_3 reacts with most of these catalysts to form stable sulfates, which destroy the catalyst activity. Several authors have considered the addition of reductants (methane, propane, propene, or LPG) in the feed composition,

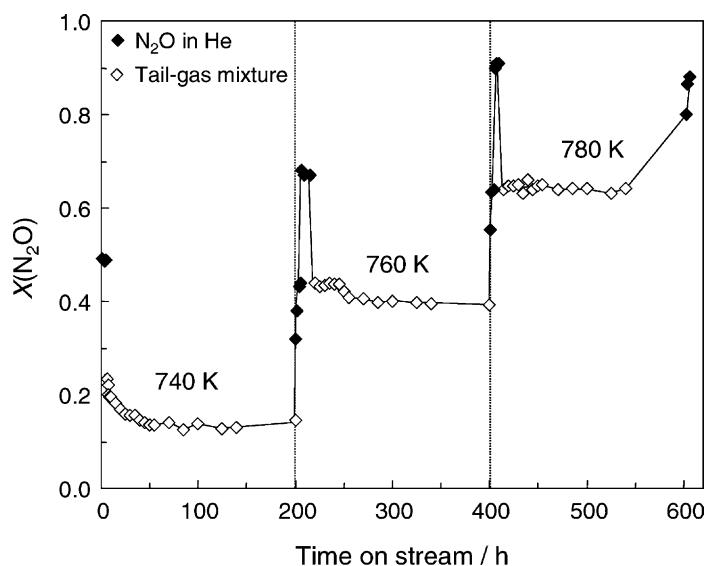


Fig. 11. N_2O conversion vs. time-on-stream over ex-FeZSM-5 in (◆) 1.5 mbar N_2O and (◇) 1.5 mbar N_2O + 120 mbar O_2 + 150 mbar CO_2 + 15 mbar H_2O + 0.75 mbar SO_2 , balance He; $P = 3$ bar; GHSV = $75\,000\text{ h}^{-1}$. Temperatures are as indicated in the figure.

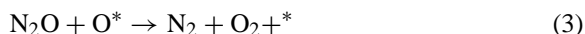
not only to promote catalytic activity of the FeMFI catalyst substantially but also to prevent the formation of sulfate species and/or increase the stability towards H_2O [11,27,33,34]. However, catalytic reduction of N_2O by addition of hydrocarbons implies an increase of the operating costs in the after-treatment, which is in principle not attractive. In addition, selective reduction of N_2O often leads to incomplete hydrocarbon combustion and high CO yields [28]. Hydrocarbon slip and CO emission can be simultaneously remedied, e.g. by incipient wetness impregnation of Pd on the FeMFI catalyst, enhancing its oxidation performance [26].

The positive effect of SO_2 on N_2O decomposition over FeZSM-5 was previously reported by some of us [12]. We have proposed that SO_2 scavenges adsorbed O^* (deposited by N_2O decomposition, reaction (1)) and thus regenerates the active site (reaction (2)):



In this study, the product gases were not analyzed for SO_3 . Centi and Vanazza [27] have recently attributed the stability of FeZSM-5 prepared by chemical vapor deposition of FeCl_3 on H-ZSM-5 towards SO_2 (using

C_3H_8 as the reductant) to the inability of the catalyst to oxidize SO_2 to SO_3 . This was concluded from the absence of SO_3 in the product gases, as determined by absorption in NaOH mixtures and analysis by ionic chromatography of the presence of sulfate ions in the solution. The remarkable stability of our ex-framework catalyst indeed suggests that SO_2 hardly chemically interacts with the catalyst surface. So SO_2 scavenges adsorbed O^* species, without formation of stable sulfates on the catalyst surface. Still, SO_2 (reaction (2)) should be a better reductant than N_2O (reaction (3)), since both reactions compete to reduce an oxidized site, regenerating it. It can tentatively be proposed that the improved N_2O conversion is caused by a favorable oxygen desorption, due to the presence of adsorbed SO_2 on the catalyst surface, as analyzed for the NO-promoted N_2O decomposition described elsewhere [41,43]:



In FeZSM-5 catalysts prepared by sublimation or (solid and liquid) ion-exchange, it seems that interaction of SO_x with the Fe sites is strong, and stable sulfate formation dramatically reduces N_2O decomposition.

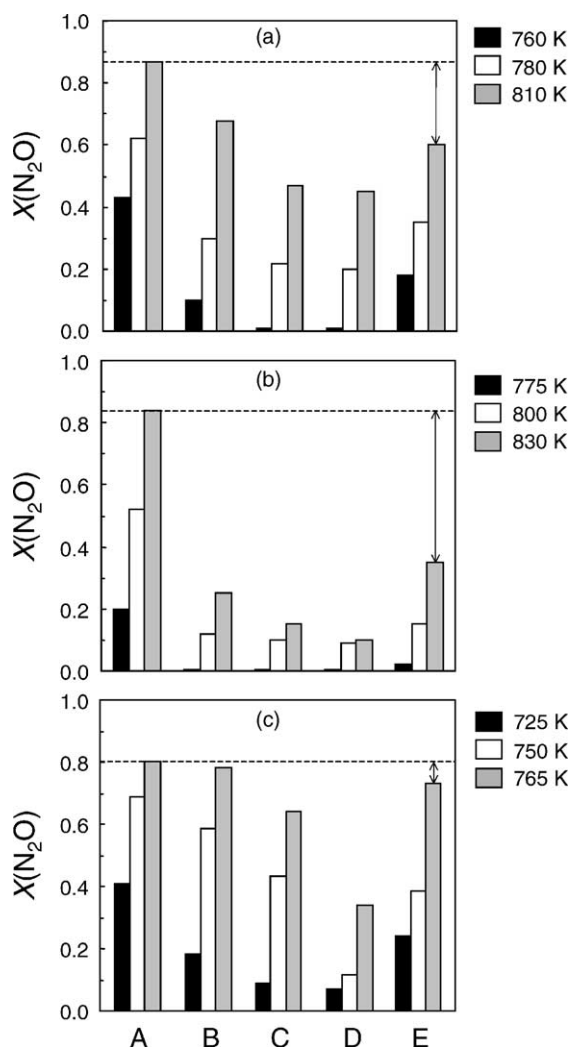


Fig. 12. N_2O conversion over (a) sie-FeZSM-5, (b) lie-FeZSM-5, and (c) sub-FeZSM-5 in (A) 1.5 mbar N_2O in He (\blacklozenge in the legend of Fig. 11), and after exposure to the complete gas mixture (\blacklozenge in the legend of Fig. 11) during (B) 1 h, (C) 5 h, and (D) 20 h, (E) as (A), 5 h after switching from the tail-gas mixture back to N_2O in He; $P = 3$ bar; GHSV = $75\,000\text{ h}^{-1}$. Temperatures are as indicated in the figure.

3.2.3. Ex-framework FeZSM-5 vs. other catalysts

The data show that a critical factor in designing catalysts for N_2O decomposition in tail-gases is to reduce the inhibition effect by oxygen, NO_x , H_2O , and SO_2 . FeZSM-5 catalysts show an extraordinary behavior, since they are not inhibited by O_2 and show an improved activity in the presence of NO

[12,22,23]. A novel ex-framework route to prepare FeZSM-5 also leads to a high stability in the presence of H_2O and SO_2 , while catalysts prepared by other preparation methods are severely inhibited and deactivated. The difference in performance of the different FeZSM-5 catalysts can be related to the preparation method, which leads to different constitutions of the catalysts with respect to dispersion, morphology, and structure of the active sites. A remarkable homogeneous distribution of highly dispersed FeO_x nano-particles of 1–2 nm in ex-FeZSM-5 is obtained by the ex-framework method. The other preparation methods fail in obtaining a homogeneous distribution of the iron oxide particles in the catalyst, as revealed by the broad FeO_x cluster size distribution indicated as Δd in Table 1. When assuming that the particles observed by TEM are responsible for N_2O decomposition activity, the lower activity of the ion-exchange and sublimation methods compared to ex-framework catalysts in N_2O decomposition could be explained. However, large FeO_x particles at the external surface of the zeolite are widely accepted to be inactive in reactions catalyzed by FeZSM-5 [25,27–31]. As shown in a previous paper [44], the ex-framework catalyst is a very heterogeneous material with respect to iron. Apart from the iron oxide nano-particles, oligonuclear oxo-iron species and isolated iron ions in the zeolite channels have been identified. This complicates the elucidation of the nature of the active sites for N_2O activation and decomposition for the observed extraordinary catalytic behavior. An attempt to determine the nature of the active sites of this catalyst for N_2O conversion is given elsewhere [45], where small oligonuclear oxo-iron species in the zeolite channels are proposed to be the active species.

Rh-catalysts (especially ex-Co-Rh, Al-HTlc) show very high initial N_2O decomposition activities, even in the presence of O_2 , NO , and H_2O . However, stability tests (600 h) show that the catalysts progressively deactivate by H_2O , and the more stable ex-FeZSM-5 system clearly overcomes their activities. Deactivation by SO_2 in Rh-based catalysts is more severe, suppressing their activity after 1 h time-on-stream. Regeneration of these catalysts by thermal treatment in inert does not lead to the recovery of the original activity. These factors limit the practical application of Rh-catalysts, and of many other formulations based on noble or transition metals.

3.3. Feasibility of the tail-gas option for N_2O abatement

3.3.1. Nitric acid plants

During the manufacture of nitric acid, N_2O is formed as an unwanted by-product in the catalytic oxidation of ammonia over the Pt–Rh gauzes. This process mostly yields the desired product NO (with selectivities of 95–97%), but also N_2O (typically 1.5–2%) and N_2 (remainder). The amount of N_2O formed depends on combustion conditions, catalyst composition and state (age), and burner design. The N_2O passes through the plant and is emitted in the tail-gas. The current technology for de- NO_x applications in nitric acid plants, i.e. the selective catalytic reduction using ammonia as a reductant and V_2O_5 -type catalysts, does not reduce N_2O emissions. Several options for N_2O destruction in nitric acid plants are currently being developed [5]. R&D efforts focus on

two locations in the plant (Fig. 13): in the ammonia burner, i.e. in process-gas options, and in the tail-gas.

In process-gas options. Different in process-gas options (in positions (a) and (b) in Fig. 13) have been considered. Efforts in position (a) focus on (i) the optimization of the design (geometry) of the Pt–Rh gauzes, or (ii) the replacement of the Pt–Rh gauzes by a metal oxide catalyst. Options to mitigate N_2O in the ammonia burner behind the gauzes (position (b)) are (iii) the homogeneous decomposition of N_2O by increasing the residence time in the ammonia burner, and (iv) catalytic N_2O decomposition after the Pt–Rh-catalyst. Options (i) and (ii) concern the optimization of the NO yields during ammonia oxidation, which indirectly leads to a lower N_2O production. All the possibilities for improvement in option (i) are not yet exhausted and currently the potential reduction of N_2O emission is uncertain. The second option, replacement of the current noble meta-based catalyst by

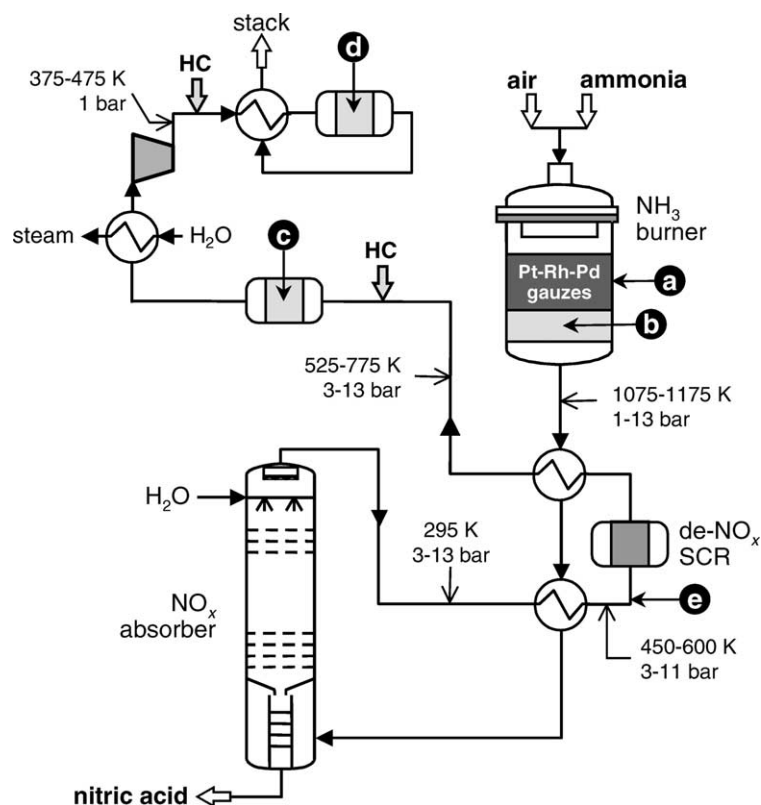


Fig. 13. Options to control N_2O emissions in nitric acid plants, with typical conditions in different locations.

a metal oxide catalyst (typically Co_3O_4), presents two major drawbacks: the ammonia conversion efficiency is substantially lower (88–92%) compared to the Pt–Rh gauzes (94–96%) under realistic conditions, and Co_3O_4 suffers from deactivation due to reduction to CoO in the upper parts of the bed [46]. Abatement of the N_2O formed in the ammonia burner is considered in options (iii) and (iv). Option (iii) implies a new reactor design [47], requiring a substantial investment in existing plants and thus prohibitive retrofit costs. Option (iv) is the most promising in this position of the plant. It involves catalytic N_2O decomposition at high temperature and for many plants would offer a simple and cost-effective way to remove N_2O . The catalyst could be easily installed in place of the Raschig rings that support the Pt–Rh gauzes and the Pd catchment. Possible drawbacks are that catalyst life may be short due to harsh conditions (temperature of 1075–1175 K and total pressure up to 13 bar) and that also the selectivity to NO decreases, since NO decomposition may be catalyzed. This would cause production losses and consequently influence the cost efficiency of the overall process dramatically. BASF reported 80 and 70% reduction of N_2O using Cu-based mixed oxide spinel during tests in dual-pressure and atmospheric pressure plants, respectively [48,49]. Norsk Hydro also developed and implemented a catalyst (based on cobalt) in a medium-sized plant of the company in March 2000, obtaining N_2O conversions >90% with NO losses <0.5% [50,51]. Other companies are also investigating this option [52–54]. In spite of the promising results of this alternative, more tests are required to determine and improve the long-term mechanical and chemical stability, activity, selectivity, product quality, and process interference.

Tail-gas options. Destruction of N_2O at a point between the outlet of the absorber and the outlet of the tail-gas expansion turbine (position (c), (d), or (e) in Fig. 13) may be a more robust option, since the conditions are less severe and these options do not interfere with the process of HNO_3 production. Application of tail-gas abatement in nitric acid plants requires high low-temperature activity in the presence of O_2 , NO_x , and H_2O . Thermal decomposition of N_2O in the tail-gas is economically unfeasible. Although a recuperative heat exchanger can be installed [55], it is likely that heat must be continuously supplied from an external source to compensate heat losses in the

system, since the diluted N_2O concentration in the tail-gas causes only a small temperature rise (e.g. the decomposition of N_2O contained in a gas at 0.15 vol.% in He leads to an adiabatic temperature rise of 6 K).

A more realistic solution is the installation of a catalytic abatement unit. Essentially, no physical limit exists (except pressure drop) for the size of the reactor. This allows the design of a reactor for very high levels of N_2O removal. A producer might also decide to install a more generously sized reactor than that immediately required, to allow for the addition of extra-catalyst later to cope with prospective N_2O emission regulations, or to optimize the catalyst requirement against the level of a greenhouse gas tax. Either direct N_2O decomposition or selective catalytic reduction of N_2O with hydrocarbons has been considered in different locations. From the point of view of catalytic activity, the best location of the after-treatment would be at the inlet of the tail-gas expansion turbine (position (b) in Fig. 13). In this location, the temperature and total pressure of the tail-gas ranges from 525 to 775 K and from 3 to 13 bar, respectively, depending on the process variant.

The use of ex-framework FeZSM-5 for direct N_2O decomposition, which shows stable N_2O conversion (>90%) at 725 K and $60\,000\text{ h}^{-1}$, appears viable in large modern high-pressure and dual-pressure plants (with high-temperature tail-gases, ranging from 725 to 775 K). This technology can contribute to greenhouse gas abatement in a cost-attractive way, since ex-FeZSM-5 does not contain any expensive noble metal and keeps a remarkable stability. The high space velocity used in this study ($60\,000\text{ h}^{-1}$) compared to a more realistic situation ($\sim 30\,000\text{ h}^{-1}$) and the relatively low pressure (3 bar vs. 4–10 bar in typical conditions) guarantee a lower operation temperature for the same N_2O conversion. Only 1/3 of the nitric acid plants in Europe have tail-gases of these characteristics, but since they are dual-pressure or high mono-pressure plants with large productions, the contribution to the capacity is certainly >60%, with equal contribution to N_2O emission.

For low-temperature tail-gases (500–525 K), typical in low (single or dual)-pressure plants, ex-FeZSM-5 would additionally require extra-heat exchange to pre-heat the feed mixture, or the addition of hydrocarbon as reducing agent. The use of hydrocarbons leads to a dramatic increase of the operation costs (four times

higher than direct N_2O decomposition), due to the high cost associated with the reductant (30–70% of the total annual cost of the abatement system) [56]. Reduction of N_2O with ammonia is also possible, but it generally requires higher temperatures than N_2O reduction with hydrocarbons [35,57]. Although ammonia is readily available in a nitric acid plant, it is probable that reduction with ammonia will not be competitive.

Temperature and pressure of the tail-gas downstream of the expander are milder (position (d) in Fig. 13), i.e. 375–475 K and 1 bar, which would require preheating of the off-gases to about 725 K by a natural-gas-fired in-line burner, as well as the addition of reducing agents to the feed mixture. Another process option that can be considered is the installation of the after-treatment upstream of the de- NO_x SCR unit (position (e) in Fig. 13). This may be favorable to improve N_2O conversion at lower temperatures, since NO promotes N_2O decomposition over ex-FeZSM-5 [20,41]. The operation temperature of a de- NO_x SCR using ammonia ranges from 575 to 725 K, depending on various parameters (type of de- NO_x catalyst, residence time, amount of ammonia injected, etc.). In this process option, care should be taken to avoid N_2O formation during NO_x reduction.

As it can be concluded from the above description, the temperature of the tail-gas is the most important

parameter that would influence the location of the catalyst unit and the abatement options. This strongly depends on the plant and should be analyzed individually in each case. Anyway, the large variety of options facilitates the search of a suitable treatment.

3.3.2. Stationary combustion processes

Fluidized-bed combustors (FBCs) of fossil fuels, biomass, and nitrogen-containing industrial or municipal waste have been developed as environmental friendly alternative for traditional forms of combustion. The low combustion temperature at which FBCs operate results in low emission levels of NO_x , which coincides with the optimal conditions for sulfur-capture. Unfortunately these merits are off-set by a strongly increased emission of N_2O [58].

In fluid-bed combustion, several locations can be identified where the ex-FeZSM-5 catalysts can be applied (Fig. 14): (a) in the bed or (b) in the freeboard, (c) after the cyclone, and (d) after the preheater. Each location requires different characteristics for a catalyst. In the combustor (positions (a) and (b)), calcined limestone and other Ca-containing materials are preferred, since they are highly thermostable and very resistant to attrition [11]. Position (c) seems to be viable for the ex-framework FeMFI catalysts, since they show high N_2O decomposition activities at the temperature of the

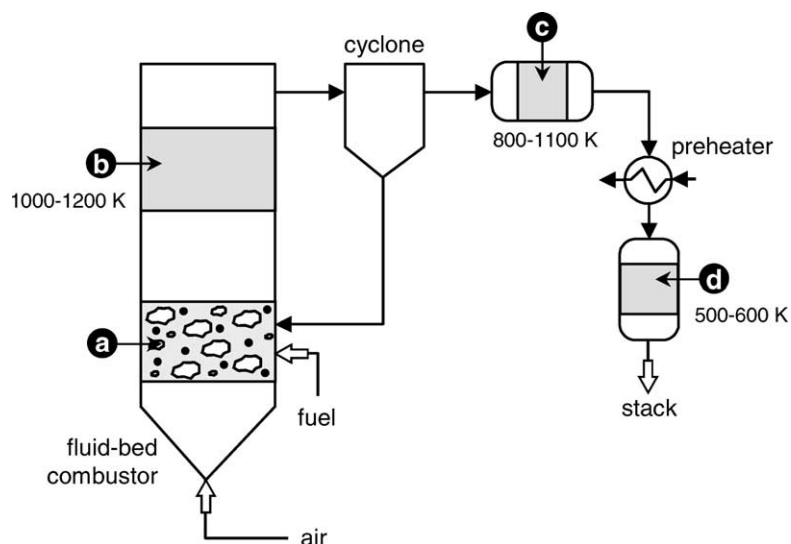


Fig. 14. Options to control N_2O emissions in fluid-bed combustors.

dust-free gas. In position (d), a high low-temperature activity is demanded, and ex-FeZSM-5 would require additionally heat exchange to preheat the feed mixture, or addition of a hydrocarbon as reducing agent. In combustion processes the major requirement for a working catalyst is the tolerance of the catalyst against deactivation by SO_2 . Ex-framework FeZSM-5 can be used for direct N_2O decomposition, due to the promotion effect of SO_2 on the reaction rate, and the stability in wet conditions (in the absence of hydrocarbons).

3.3.3. Other N_2O sources

Other “newly identified” sources of N_2O from chemical production plants where a catalytic abatement can be used effectively are the production of acrylonitrile, caprolactam, glyoxal, and in general organic syntheses using HNO_3 as an oxidant or processes involving ammonia oxidation. Acrylonitrile, precursor of nylon 6,6 and copolymers like SAN (styrene acrylonitrile) or ABS (acrylonitrile–butadiene–styrene), is produced by ammoxidation of propylene with ammonia and oxygen in a fluidized-bed catalytic reactor. This process generates N_2O during ammonia combustion, in a similar way to the case described during nitric acid manufacture. However, no data on concentrations, temperatures, and emissions have been reported. Substantial amounts of N_2O are formed during the production of

ammonia-derived hydroxylamine, an intermediate in the manufacture of caprolactam (monomer for nylon 6 fibers and plastics). This tail-gas contains N_2O (usually in high concentration), NO_x , H_2O , SO_2 , HCN , and NH_3 . N_2O concentration in the tail-gas can largely vary (from 500 ppm to 60 vol.% in Dutch caprolactam plants), depending on the process variant [59]. Concentrated N_2O off-gas is produced during the manufacture of glyoxal (intermediate in the production of copolymers, pharmaceuticals, resins, pesticides, etc.) by reaction between acetaldehyde and nitric acid. In this case, N_2O is accompanied by NO_x , O_2 and H_2O .

The high N_2O concentration in these tail-gases (even up to 60 vol.%), resembles the situation for adipic acid plants, and should in principle make extrapolation of developed technologies (see [9,10]) from this source straightforward. The recovery of the large amount of concentrated N_2O as a selective oxidant is an option, but the utility of the product (e.g. phenol) in the plant of its surroundings may be limited. In these cases different end-of-pipe technologies have been developed. Control of the exotherm of N_2O decomposition is a notable design parameter in catalytic/thermal units to abate this gas. Diluting the tail-gas is an efficient way to deal with this issue. Clarian in cooperation with IRMA have recently installed a N_2O decomposition unit at a glyoxal production site using an ion-exchanged Fe-ferrierite

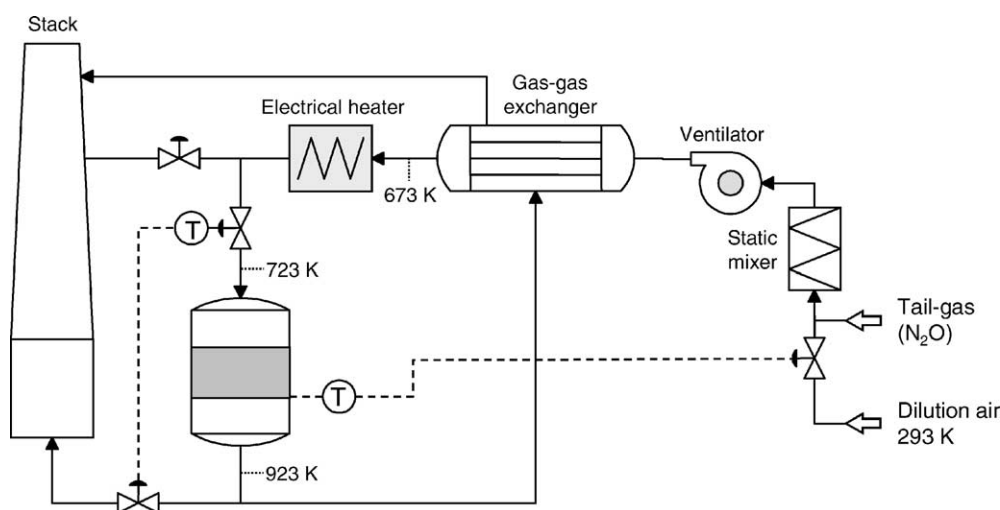


Fig. 15. Flow sheet of the N_2O abatement treatment in a glyoxal production unit (adapted from [56]).

catalyst [60,61]. In this treatment, shown in Fig. 15, the N_2O in the tail-gas is diluted from 85 to 10 vol.% by air at the inlet of the process, in order to control properly the exothermicity of the reaction and to suit the catalyst stability [60]. The adiabatic temperature rise in the reactor is ~ 200 K, which is used to preheat the incoming tail-gas up to 675 K. The same concept can be applied using ex-FeZSM-5 in these sources, in view of the excellent catalytic activity and stability.

3.4. Catalyst and reactor design

Laboratory screening and testing is carried out with a catalyst powder or pellets. Small particles normally do not apply in conventional industrial fixed-bed reactor because of the high-pressure drop. The implementation of any catalytic N_2O abatement unit in stationary sources (chemical production or combustion processes) requires a close look to the reactor type, in order to achieve maximum yields under efficient and safe operation. The practical form and shape of the catalyst is a crucial aspect to obtain reliable design data for full-scale implementation. Because of the demand for increase in conversion, selectivity, and energy efficiency, the chemical reactor of the 21st century will be characterized, at least for high space velocity applications, by the presence of “structure” on all length scales.

In this paragraph, a numerical comparison between a fixed-bed reactor with shaped particles (extrudates) and monolithic reactor with structured catalysts is pre-

sented (Fig. 16a and b, respectively). This is exemplified for the catalytic decomposition of N_2O upstream of the tail-gas expander in nitric acid plants (position (c) in Fig. 13). For the calculation, the activity data of ex-FeZSM-5 in the simulated tail-gas mixture in Fig. 4 were used.

Table 2 shows the dependency of reactor volume, effectiveness factor, and pressure drop of both geometries. The general expressions used can be found in reviews and textbooks [62–64] and more specifically in an upcoming publication [65]. The calculations were carried out for a nitric acid plant of a capacity of 1500 t HNO_3 per day and a volumetric flow of the tail-gas of $2 \times 10^5 \text{ Nm}^3 \text{ h}^{-1}$. Two extreme pressures upstream of the expander were used: 4 and 10 bar. An allowable pressure drop of 200 mbar was fixed, with a reactor diameter of 2 m. N_2O conversion of 80% ($X = 0.8$) was targeted at reaction temperature of 750 K.

Fixed-bed reactor. Due to the high intrinsic reaction rates, the reaction in common particles will exhibit severe diffusion limitations (effectiveness factor of 20–35% with extrudates of 6 mm). Only the outer part of the particle is used for the reaction, which in turn would call for small catalyst particles. However, these lead to a severe pressure drop. At low pressure, none of the particle sizes used satisfies the criterion of pressure drop allowance, even for particles of 10 mm (not shown). This is due to the corresponding increased space time in the reactor at a lower total pressure. Reactor volumes ranging from 3 to 5 m^3 are required with extrudates of 6 mm for the required

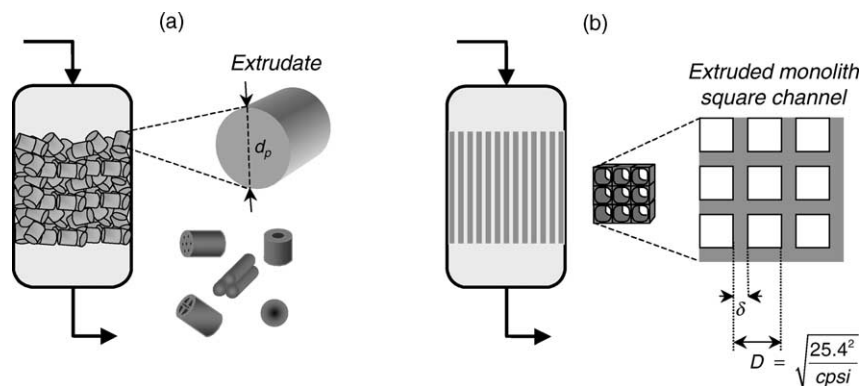




Fig. 16. Schematic representation of (a) a fixed-bed reactor and (b) a monolithic reactor. Design reactor parameters are extrudate size (d_p) in the fixed bed and wall thickness (δ) and cell pitch (D) in the monolith. D is related with the cell density, normally expressed as cpsi (cells per square inch).

Table 2

Comparison of reactors for direct N₂O decomposition over ex-FeZSM-5 in tail-gas of nitric acid plants (upstream of the expander, see Fig. 13c; basis of design are defined in the text)

Parameter	Fixed-bed reactor		Monolithic reactor	
Type	Extrudates		Extruded monolith (square channels)	
Geometry	$d_p = 6$ mm, 		200 cpsi, $d = 0.4$ mm, 	
Pressure (bar)	4	10	4	10
Reactor volume (m ³)	5	3	2.2	1
Bed height (m)	0.8	0.5	0.7	0.3
Catalyst effectiveness, η (–) ^a	0.33	0.21	0.95	0.88
Pressure drop (mbar)	630	160	60	10

^a This factor indicates the catalyst utilization in the reactor, defined as the ratio between the observed reaction rate and the rate without gradients.

N₂O conversion. Setting higher N₂O conversion targets or operation at lower temperatures is impractical using this design. Obviously, the requirements are more difficult to meet if a lower maximum pressure drop is required.

Monolithic reactor. For gas phase applications, typically using high space velocities, structured catalysts are very convenient [64,66]. In the current case monolithic structures allow the combination of high intrinsic activity, high catalyst effectiveness, and a low-pressure drop. Decoupling of the hydrodynamics, kinetics, and transport phenomena can be achieved by structured catalysts [67]. There is a wide range of commercially available monolithic structures, which makes the reactor monolith selection quite flexible. An optimal design is proposed, since using a high cell density and a large wall thickness leads to low reactor volumes, increased pressure drop and decreased catalyst effectiveness. We have considered here extruded monoliths with the ex-FeZSM-5 catalyst. A standard monolith of 200 cpsi and $\delta = 0.4$ mm leads to high effectiveness ($\sim 90\%$), small reactor volumes (1.0 and 2.5 m³, at 10 and 4 bar, respectively), and low-pressure drop (<100 mbar). The high effectiveness obtained contrasts with the low values in the packed-bed reactor, $<40\%$ for a proper particle/extrudate size. The reactor volume required depends on the cell density and wall thickness, being even smaller in magnitude as required for a fixed bed. This clearly indicates that the high catalyst effectiveness in a monolith compensates for the lower amount of catalyst as compared to a fixed-bed reactor. Another major advantage is the low-pressure drop of the monolith structure, due to the relative open

frontal area in the channels. From the reactor volume, bed heights of 0.3 and 0.7 m are derived (the reactor diameter is fixed at 2 m). Another valuable advantage of the monolithic reactor compared to the fixed-bed reactor is the flexibility for operation under different requirements of pressure and conversion, without violating operational constraints, e.g. by doubling the reactor height 99% conversion is achieved at a pressure drop of 40 mbar.

The structured reactor concept is optimal for N₂O removal in nitric acid plants, not only for catalytic N₂O decomposition or reduction in the tail-gas, but also in the in process-gas catalytic N₂O decomposition (position (b) in Fig. 13). In the latter case, much higher reaction rates are expected due to the temperature and pressure. Therefore, external mass transfer controls the process. From our calculations assuming gas phase and laminar flow in the channels, it is concluded that a monolithic geometry provides sufficiently high activities [65].

The monolithic catalyst for N₂O abatement in stationary sources can be implemented as shown in Fig. 17. The monolith catalyst, typically in square units of ca. 150 mm \times 150 mm, can be packed in catalyst baskets, which are inserted in catalyst layers. A typical practice in the reactor design to allow flexible operation (prospective or more stringent regulations or operation changes in the plant) consists of leaving spare space for an extra layer of catalyst. The possible addition of reductant is also considered in the figure. The vast commercial experience gained in de-NO_x NH₃-SCR [68,69], can be extrapolated to the design and implementation of this system.

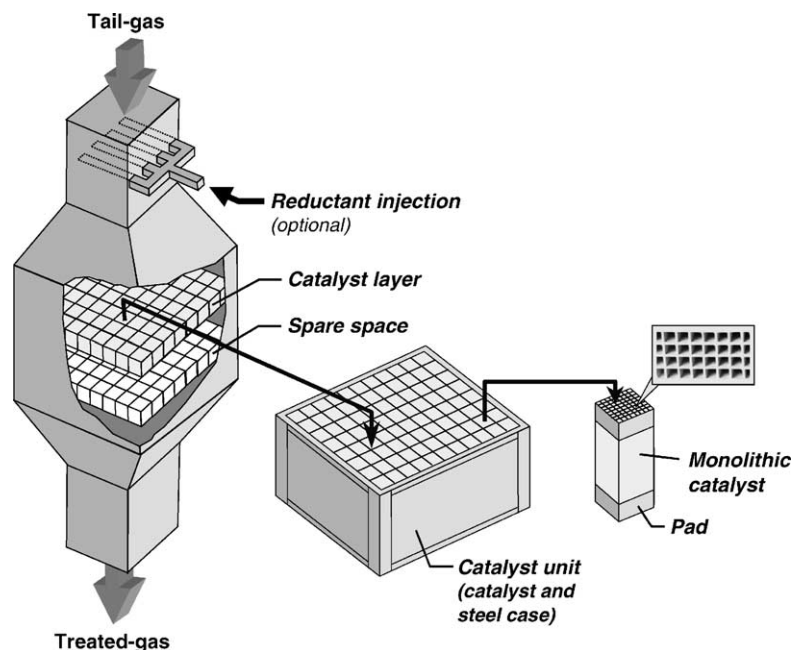


Fig. 17. Reactor and catalyst design for N_2O abatement options in tail-gases from stationary sources.

Structured reactors can be effectively applied in the other sources discussed previously. This specially applies to combustion processes (see Fig. 14), where a high dust and erosion tolerance are essential requirements in the reactor design. In chemical processes with concentrated N_2O streams, the thermostability is a key aspect for the successful application of monoliths.

Other reactor configurations. As an alternative reactor configuration with low-pressure drop, “lateral flow” type modules based on the fixed-bed concept can also be considered. This reactor concept has been developed by CRI Catalysts and Shell Research, for example de- NO_x SCR with ammonia in nitric acid plants using Ti–V based catalysts [70]. The modules, filled with catalyst particles of 1–2 mm, are hoisted into the reactor housing and placed on top of a support grid. This grid holds the weight of the modules, but it also provides a gas tight sealing between the modules and the grid. The gas passes the module only once, and the gas flow maybe in an upward, downward, or horizontal direction. In this reactor the total cross-sectional bed area is larger than the reactor diameter, and thus pressure drop is minimized. The effectiveness of the small catalyst particles, is largely improved compared

to a conventional fixed-bed reactor. The disadvantage of this system is the increased reactor volume compared to the monolithic reactor (by a factor of 2–3). In addition, dust and erosion resistance are much less favorable than in monoliths, where a large open frontal area is present.

4. Conclusions

An ex-framework preparation route leads to active and stable FeZSM-5 catalyst for direct N_2O decomposition in simulated tail-gases (containing O_2 , NO , CO_2 , H_2O and SO_2). This result indicates a great potential of this catalytic system for commercial applications, in tail-gases from nitric acid plants and combustion processes in fluid-bed reactors. Other applications include caprolactam, glyoxal, and acrylonitrile production plants. The superior performance (activity and stability) of the ex-framework catalyst compared to FeZSM-5 catalysts prepared by conventional (solid and liquid)-ion-exchanged and sublimation methods indicates a crucial role of the preparation method on the formation of the active sites in N_2O

decomposition. Noble-metal based catalysts, although showing very high activities in a $\text{N}_2\text{O}/\text{He}$ feed (especially ex-Co–Rh, Al-HTlc), are severely inhibited by NO , H_2O , and SO_2 , and suffer from deactivation during time-on-stream. This limits their application in tail-gas situations. Monolithic reactors are optimal for implementation of the catalyst in the tail-gas unit, since they allow the combination of high intrinsic activity, high catalyst effectiveness, and low-pressure drop.

Acknowledgements

This research was financially supported by the Dutch Council for Chemical Research (CW/NWO).

References

- [1] P.J. Crutzen, *J. Geophys. Res.* 76 (1971) 7311.
- [2] P.J. Crutzen, C.J. Howard, *Pure Appl. Geophys.* 116 (1978) 497.
- [3] L. Donner, V. Ramanathan, *J. Atmos. Sci.* 37 (1980) 119.
- [4] V. Ramanathan, R.J. Cicerone, H.H. Singh, J.T. Kiel, *Geophys. J. Res.* 90 (1985) 5547.
- [5] J. Pérez-Ramírez, Catalyzed N_2O activation. promising (new) catalysts for abatement and utilization, Ph.D. Thesis, Delft University of Technology, The Netherlands, 2002.
- [6] C. Kroeze, Nitrous oxide emission inventory and options for control in the Netherlands, Report No. 773001004, National Institute for Public Health and the Environment, Bilthoven, The Netherlands, 1994.
- [7] G. Centi, S. Perathoner, F. Vanazza, *Chemtech* 12 (1999) 48.
- [8] G. Centi, S. Perathoner, F. Vanazza, M. Marella, M. Tomaselli, M. Mantegazza, *Adv. Environ. Res.* 4 (2000) 325.
- [9] R.A. Reimer, C.S. Slaten, M. Seapan, M.W. Lower, P.E. Tomlinson, *Environ. Prog.* 13 (1994) 134.
- [10] R.A. Reimer, C.S. Slaten, M. Seapan, T.A. Koch, V.G. Triner, in: J. van Ham, A.P.M. Baede, L.A. Meyer, R. Ybema (Eds.), *Non- CO_2 Greenhouse Gases: Scientific Understanding, Control and Implementation*, Kluwer Academic Publishers, Dordrecht, 2000, pp. 347–358.
- [11] F. Kapteijn, J. Rodríguez-Mirasol, J.A. Moulijn, *Appl. Catal. B* 9 (1996) 25.
- [12] F. Kapteijn, G. Mul, G. Marbán, J. Rodríguez-Mirasol, J.A. Moulijn, in: J.W. Hightower, W.N. Delgass, E. Iglesia, A.T. Bell (Eds.), *Studies in Surface Science and Catalysis*, vol. 101, 1996, p. 641.
- [13] J.N. Armor, T.A. Braymer, T.S. Farris, Y. Li, F.P. Petrocelli, E.L. Weist, S. Kannan, C.S. Swamy, *Appl. Catal. B* 7 (1996) 397.
- [14] T.W. Dann, K.H. Schulz, M. Mann, M. Collings, *Appl. Catal. B* 6 (1995) 1.
- [15] X.F. Wang, H.C. Zheng, *Appl. Catal. B* 3 (1993) 55.
- [16] J. Oi, A. Obuchi, G.R. Bamwenda, A. Ogata, H. Yagita, S. Kushiyaama, K. Mizuno, *Appl. Catal. B* 12 (1997) 277.
- [17] G. Centi, A. Galli, B. Montanari, S. Perathoner, A. Vaccari, *Catal. Today* 35 (1997) 113.
- [18] J. Oi, A. Obuchi, A. Ogata, G.R. Bamwenda, K. Tanaka, T. Hibino, S. Kushiyaama, *Appl. Catal. B* 13 (1997) 197.
- [19] J. Pérez-Ramírez, J. Overeijnder, F. Kapteijn, J.A. Moulijn, *Appl. Catal. B* 23 (1999) 59.
- [20] J. Pérez-Ramírez, F. Kapteijn, J.A. Moulijn, *Catal. Lett.* 60 (1999) 133.
- [21] H.C. Zheng, X.Y. Pang, *Appl. Catal. B* 13 (1997) 113.
- [22] F. Kapteijn, G. Marbán, J. Rodríguez-Mirasol, J.A. Moulijn, *J. Catal.* 167 (1997) 256.
- [23] J. Pérez-Ramírez, F. Kapteijn, G. Mul, J.A. Moulijn, *Chem. Commun.* (2001) 693.
- [24] J. Pérez-Ramírez, F. Kapteijn, G. Mul, J.A. Moulijn, *Appl. Catal. B* 35 (2002) 227.
- [25] M. Rauscher, K. Kesore, R. Mönnig, W. Schwieger, A. Tibler, T. Turek, *Appl. Catal. A* 184 (1999) 249.
- [26] R.W. van den Brink, S. Booneveld, J.R. Pels, D.F. Bakker, M.J.F.M. Verhaak, *Appl. Catal. B* 32 (2001) 73.
- [27] G. Centi, F. Vanazza, *Catal. Today* 53 (1999) 683.
- [28] M. Kögel, R. Mönnig, W. Schwieger, A. Tisser, T. Turek, *J. Catal.* 182 (1999) 470.
- [29] R. Joyner, M. Stockenhuber, *J. Phys. Chem. B* 103 (1999) 5963.
- [30] H.-Y. Chen, W.M.H. Sachtler, *Catal. Today* 42 (1998) 73.
- [31] G.I. Panov, A.K. Uriarte, M.A. Rodkin, V.I. Sobolev, *Catal. Today* 41 (1998) 365.
- [32] A. Ribera, I.W.C.E. Arends, S. de Vries, J. Pérez-Ramírez, R.A. Sheldon, *J. Catal.* 195 (2000) 287.
- [33] Z.S. Rak, M.J.F.M. Verhaak, A. Bos, G. Centi, ECN, WO 99/49954.
- [34] C. Pophal, T. Yogo, K. Yamada, K. Segawa, *Appl. Catal. B* 16 (1998) 177.
- [35] M. Mauvezin, G. Delahay, F. Kibich, B. Coq, S. Kieger, *Catal. Lett.* 62 (1999) 41.
- [36] J. Pérez-Ramírez, R.J. Berger, G. Mul, F. Kapteijn, J.A. Moulijn, *Catal. Today* 60 (2000) 93.
- [37] K. Yuzaki, T. Yarimizu, K. Aoyagi, S. Ito, K. Kunimori, *Catal. Today* 45 (1998) 119.
- [38] J. Pérez-Ramírez, G. Mul, J.A. Moulijn, *Vib. Spectrosc.* 27 (2001) 75.
- [39] J. Pérez-Ramírez, G. Mul, F. Kapteijn, J.A. Moulijn, *J. Mater. Chem.* 11 (2001) 821.
- [40] J. Pérez-Ramírez, G. Mul, F. Kapteijn, J.A. Moulijn, *J. Mater. Chem.* 11 (2001) 2529.
- [41] J. Pérez-Ramírez, F. Kapteijn, G. Mul, J.A. Moulijn, *J. Catal.* 208 (2002) 211.
- [42] J. Pérez-Ramírez, J.M. García-Cortés, F. Kapteijn, M.J. Illán-Gómez, A. Ribera, C. Salinas-Martínez de Lecea, J.A. Moulijn, *Appl. Catal. B* 25 (2000) 191.
- [43] G. Mul, J. Pérez-Ramírez, F. Kapteijn, J.A. Moulijn, *Catal. Lett.* 7 (2001) 77.
- [44] J. Pérez-Ramírez, G. Mul, F. Kapteijn, J.A. Moulijn, A.R. Overweg, A. Doménech, A. Ribera, I.W.C.E. Arends, *J. Catal.* 207 (2002) 113.

- [45] J. Pérez-Ramírez, F. Kapteijn, J.C. Groen, A. Doménech, G. Mul, J.A. Moulijn, *J. Catal.* (2002), submitted for publication.
- [46] J. Petryk, E. Kolakowska, *Appl. Catal. B* 24 (2000) 121.
- [47] E. Fareid, G. Kongshaug, L. Hjørnevik, O. Nirisen, *Norsk Hydro*, EP 0359286A2 (1993).
- [48] G. Kuhn, V. Schumacher, E. Wagner, *Proceedings of the International Fertilizer Society*, vol. 435, 1999, p. 1.
- [49] V. Schumacher, G. Bürger, T. Fetzer, M. Baier, M. Hesse, BASF, DE 19819882A1 (1999).
- [50] T. Hallan, O. Nirisen, K. Schöffel, D. Waller, in: *Proceedings of the International Conference on Industrial Atmospheric Pollution, NO_x–N₂O Emission Control: Panel of Available Techniques*, ADEME Editions, Paris, 2001 (Session 4).
- [51] O. Nirisen, K. Schöffel, D. Waller, D. Øvrebo, *Norsk Hydro*, WO 02/02230A1 (2002).
- [52] T. Koch, DuPont, US 5 478 549 (1995).
- [53] P. Vernooy, DuPont, WO 00/51715 A1 (2000).
- [54] R. Kubisa, M. Klein, L&C Steinmüller, WO 99/07638 (1999).
- [55] M. Galle, D.W. Agar, W. Watzemberger, *Chem. Engng. Sci.* 56 (2001) 1587.
- [56] R.W. van den Brink, in: *Proceedings of the International Conference on Industrial Atmospheric Pollution, NO_x–N₂O Emission Control: Panel of Available Techniques*, ADEME Editions, Paris, 2001 (Session 1).
- [57] B. Coq, M. Mauvezin, G. Delahay, J.B. Butet, S. Kieger, *Appl. Catal. B* 27 (2001) 193.
- [58] M.A. Wójtowicz, J.R. Pels, J.A. Moulijn, *Fuel Process. Technol.* 34 (1993) 1.
- [59] W. Glasz, Personal communication, 2001.
- [60] C. Harmon, P. Janssens, in: *Proceedings of the International Conference on Industrial Atmospheric Pollution, NO_x–N₂O Emission Control: Panel of Available Techniques*, ADEME Editions, Paris, 2001 (Session 7).
- [61] B. Neveu, C. Harmon, K. Malefant, WO 99/34901 (1999) Grande Paroisse.
- [62] G.F. Froment, K.B. Bischoff, *Chemical Reactor Analysis and Design*, 2nd ed., Wiley, New York, 1990.
- [63] L.K. Doraiswamy, M.M. Sharma, *Heterogeneous Reactions: Analysis, Examples, and Reactor Design*, vol. 1, Gas–Solid and Solid–Solid Reactions, Wiley, New York, 1984.
- [64] A. Cybulski, J.A. Moulijn, *Catal. Rev.-Sci. Eng.* 36 (1994) 179.
- [65] J. Pérez-Ramírez, F. Kapteijn, J.A. Moulijn, in preparation.
- [66] R.M. Heck, R.J. Farrauto, *Catalytic Air Pollution, Commercial Technology*, Van Nostrand Reinhold, New York, 1995.
- [67] F. Kapteijn, J.J. Heiszwolf, T.A. Nijhuis, J.A. Moulijn, *Cattech* 3 (1999) 24.
- [68] <http://www.khi.co.jp/products/sanki/plantchem/nox.htm>.
- [69] A. Beretta, E. Tronconi, G. Groppi, P. Forzatti, in: A. Cybulski, J.A. Moulijn (Eds.), *Structured Catalysts and Reactors*, Marcel Dekker, New York, 1998, pp. 121–148.
- [70] <http://www.cri-catalysts.com/de-nox.htm>.